Journal of Power Sources 188 (2009) 192–198

Contents lists available at ScienceDirect

Journal of Power Sources

journal homepage: www.elsevier.com/locate/jpowsour

Optimisation of carbon nanofiber based electrodes for polymer electrolyte membrane fuel cells prepared by a sedimentation method

Eva Wallnöfer[a,*], Markus Perchthaler[a], Viktor Hacker[a], Gaetano Squadrito[b]

[a] Department of Chemical Engineering and Environmental Technology, CD-Laboratory for Fuel Cell Systems, Graz University of Technology, Graz, Austria
[b] Consiglio Nazionale delle Ricerche, Istituto di Tecnologie Avanzate per l'Energia, Via Salita S. Lucia sopra Contesse n. 5, 98126 S. Lucia, Messina, Italy

ARTICLE INFO

Article history:
Received 11 June 2008
Received in revised form 23 October 2008
Accepted 16 November 2008
Available online 21 November 2008

Keywords:
Polymer electrolyte membrane fuel cell (PEMFC)
Carbon nanofibers (CNFs)
Electrode preparation
Sedimentation method
Electrode optimisation
Platinum catalyst

ABSTRACT

Tubular carbon nanofibers with an average diameter of 150 nm are investigated as a possible material for the electrodes preparation for polymer electrolyte membrane fuel cells. Well-dispersed platinum particles with an average crystallite size of 4.6 nm are deposited on surface-oxidised fibers to be used as a catalyst support with an electroless plating method. The carbon nanofiber-based electrodes are prepared by a sedimentation method without the use of organic solvents. This method allows an exact setting of the fiber and binder content and the catalyst loading. The electrodes are optimised by varying the thickness of the gas diffusion layer and its binder content as well as the thickness of the active layer. These optimised electrodes show a considerably better performance when compared to carbon black-based electrodes with the same catalyst loading prepared by a spraying process using the same type and amount of electrolyte in the membrane electrode assembly. By reducing the platinum content from 0.7 to 0.2 mg cm^{-2}, catalyst utilisation is significantly increased.

1. Introduction

Fuel cells have attracted much attention for their potential as clean power sources. Usually, carbon black is used as low temperature fuel cell electrode material, but carbon nanofibers (CNFs) with different structures have also already been used or considered for use as alternative electrode material in polymer electrolyte membrane fuel cells (PEMFCs) [1–11], direct methanol fuel cells (DMFCs) [12–26], alkaline fuel cells (AFCs) [27,28] and even in direct ethanol fuel cells [29]. The deposition of the catalyst metal on the CNFs, mostly platinum or its alloys, is associated with the studies concerning fuel cell applications but it is also an independent research subject. The research activities achieved excellent results with impregnation methods and the reduction of metal salts with hydrogen [5–7,14,15,30–33] or thermal treatment [30], sputtering [23], electrochemical metal plating on CNF electrodes [19] as well as the use of reducing agents like ethylene glycol [3–5,16–18,21,26,34–36], $NaBH_4$ [2,27] and others [7,17]. In these studies, different kinds of CNFs were investigated. Most of them describe the use of carbon nanotubes, which occupy a relevant position due to their perfect structure and unique mechanical and electrical properties, but other kinds of CNFs with a different structure, diameter and aspect of the carbon particles have also been used for fuel cell applications [2,6,7,13–15,26,37]. The benefits which are expected from the application of CNFs in the active layer and/or in the gas diffusion layer of fuel cell electrodes are a higher thermal and electrical conductivity, better mechanical properties, and a higher electrochemical and chemical stability of the electrodes under fuel cell operating conditions. Furthermore, the structure of the CNFs influences catalyst utilization, the gas diffusion and the wetting behaviour of the electrolyte. The electrode preparation methods commonly used for spherical, carbon black material are also suitable for CNF material, even though process parameters have to be adapted. CNF electrodes have been fabricated mostly by spraying [3,7,17] and brushing [2,8,30,38], but also by rolling [27], sedimentation [28], electrophoresis [19] and chemical vapour deposition methods [23].

Previously, tubular CNFs with an average diameter of 150 nm were successively used in cathodes for AFCs [27,28]. The aim of this work was to use these tubular CNFs as PEMFC electrode and catalyst support material and to optimise the electrodes for this application. Therefore, the influence of the thickness of the gas diffusion layer and the active layer as well as the influence of the binder content of the gas diffusion layer on the CNF electrode performance was investigated. In a following step, the catalyst loading of the electrodes was optimised to reach a maximum platinum utilisation. The electrodes were prepared by a sedimentation process. A comparison between carbon black and CNFs as catalyst support and gas

* Corresponding author. Tel.: +43 316 873 8786; fax: +43 316 873 8782.
E-mail address: eva.wallnoefer@tugraz.at (E. Wallnöfer).

0378-7753/$ – see front matter © 2008 Elsevier B.V. All rights reserved.
doi:10.1016/j.jpowsour.2008.11.052

diffusion media was carried out with carbon black-based sprayed electrodes.

2. Experimental

2.1. CNF purification and platinum deposition

The purification step of raw tubular CNFs (HTF150FF-LHT, Electrovac AG, Austria) with an average diameter of 150 nm was performed in a mixture of concentrated nitric acid (65% vol.) and sulphuric acid (98% vol.) at a ratio of 3:2 (0.25 g CNFs per 100 ml) under refluxing conditions for 10 h [28]. Purified CNFs were dispersed in distilled water with an ultrasonic processor for further treatment. Platinum deposition was carried out with the reduction of the required amount of H_2PtCl_6 (aqueous solution, 10 g l^{-1}), added within 5 s under vigorous stirring to an alkaline CNF dispersion (0.25 g CNFs per 100 ml), which contained dissolved $NaBH_4$ in excess (10 mg $NaBH_4$ per 1 mg Pt). The reaction was carried out under stirring at 3 °C for 48 h. A pH-value of 12 was adjusted with NH_4OH. After the reduction, the product was filtered, washed with distilled water and dried at 100 °C for 12 h [28]. The platinum loading was varied from 3.3 up to 24 wt%, depending on the required thickness and platinum loading of the electrode, and was adjusted with the amount of H_2PtCl_6 and controlled by weighting.

Platinum crystallite size was examined on CNFs loaded with 17 wt% platinum with X-ray diffraction (XRD, Philips PW3710, Cu anode). Furthermore, the platinum particles deposited on CNF surfaces were examined with scanning electron microscopy (SEM, ZEISS DSM 982 Gemini and JEOL JWS-7515) and transmission electron microscopy (TEM, Philips CM12).

2.2. Electrode and MEA preparation

For the preparation of CNF-based electrodes, a sedimentation process already used for AFC cathodes in our previous work [28] was chosen. This fast and simple process enabled the production of highly-reproducible gas diffusion layers (GDLs) and active layers (ALs) without the use of organic solvents. As a binder and hydrophobic agent, polytetrafluorethylene (PTFE) was used. To fabricate the GDL, the required amount of CNFs and PTFE (Dyneon^{TM}, TF 5035 PTFE) was dispersed in distilled water. As a support, a fitting piece of carbon paper (Sigracet GD Media GDL 24 BA, 190 μm thickness) was placed on a frit and the solid components of the dispersion were sedimented on it. The AL was sedimented on the GDL in the same way, using platinum-loaded CNFs instead. After a sintering step, the electrodes were wetted on the AL side with a 33 wt% of Nafion electrolyte in respect to the platinum-loaded CNFs by a spraying process using a Nafion solution (5 wt%) from Fluka Chemika, cut into pieces and pressed with fitting pieces of N115 membranes to form the membrane electrode assemblies (MEAs) at 120 °C for3 min. The MEAs were inserted into a fuel cell with an active area of 5 cm^2 and serpentine flow field channels (channel width: 0.5 mm at the anode side and 1.0 mm at the cathode side).

The optimisation of the electrodes was carried out by varying successively the thicknesses of the AL and the GDL by varying the CNF loading as well as the GDL binder content. In our previous work, these parameters considerably influenced the performance of AFC cathodes [28]. The platinum loading of the anode and the cathode was kept constant (0.7 mg cm^{-2}) and both electrodes of each MEA were similar in design in these optimisation steps. The AL binder content was kept constant and as low as possible with 7 wt% of the CNFs, because the added solid electrolyte worked as an additional binder and the wetting with the electrolyte in the AL is not dependent on the PTFE content as it is in the case of a liquid electrolyte. Table 1 shows the electrode parameters of the investigated MEAs. Because of the constant platinum content of the electrodes, the platinum loading of the CNFs used as catalyst support had to be different at different AL thicknesses.

After the optimisation of the GDL and the AL, the catalyst loading of the cathode and the anode was reduced. When lowering the platinum loading of the optimised electrodes, there was the option of either keeping the platinum loading of the CNFs as a constant, which would result in thinner ALs, or keeping the CNF loading of the AL constant, which would result in lower platinum loadings of the CNFs. Three different MEAs were realised with each of the two options; the platinum loading of the cathodes was lowered to 0.4 mg cm^{-2} and combined with anodes with 0.4, 0.2 and 0.1 mg cm^{-2} platinum (see Table 2). The GDL of each electrode was manufactured with an optimal CNF and binder content (12.3 mg cm^{-2} CNFs and 21 wt% PTFE). The performances of these MEAs were investigated and compared to the MEA with a catalyst loading of 0.7 mg cm^{-2}.

To compare the CNFs with carbon black as catalyst support, electrodes consisting of carbon black with 0.7 mg cm^{-2} platinum were prepared by a spraying process and formed to an MEA using a N115 membrane and the same amount of Nafion in the AL as used in the case of sedimented CNF-based electrodes. The GDL was prepared with Vulcan carbon VC XC 72 and 17 wt% PTFE, sprayed on the same type of carbon paper used in the sedimentation process. To prepare the AL, a carbon black catalyst support (20 wt%, Quintech C-20-PT) was dispersed in the required amount of the Nafion solution and sprayed on the GDL. The performance of this MEA was compared to the optimised MEAs with CNF-based electrodes with different platinum loadings.

2.3. Test conditions

The gas flows of hydrogen and air or oxygen with a 90% relative humidity and ambient pressure were controlled with stochiometric values of 1.2 at the anode and 2.2 at the cathode. The cell temperature was 70 °C. MEAs were activated at 0.6 and 0.4 V (alternating, 30 min each) for 4 h with oxygen. Polarisation curves and cyclic voltammograms (CVs) were recorded with a Zahner IM6ex electrochemical workstation and a Zahner PP240 potentiostat. The step rate of the polarisation curves was 10 mV s^{-1}. To investigate the specific active catalyst surface of the electrodes, CVs were recorded between 0.03 and 1.4 V with a step rate of 100 mV s^{-1} and four cycles per measurement, whereas the electrode was fed by hydrogen (50 ml min^{-1}) and the other electrode of the MEA by nitrogen (50 ml min^{-1}).

3. Results and discussion

3.1. CNF purification and platinum deposition

In addition to the removal of catalyst metals and the reduction of non-fibrous carbon that resulted in a weight loss of about 10%, the CNF purification step also induced oxygen-containing functional groups on the CNF surfaces, which are expected to lead to a significantly better platinum metal deposition [39,40]. Furthermore, acid-treated CNFs were easier to disperse in water without the use of surfactants. However, non-acid treated CNF material showed a tendency both to sedimentate and to float on the surface.

With the results of the XRD analysis, an average platinum crystallite size of 4.6 nm could be calculated from the Pt (2 2 0) peak at 67.8° 2Θ which was not disturbed by the graphite signal (see Fig. 1 and Table 3). Images of SEM and TEM analyses (Figs. 2 and 3; CNFs loaded with 19 wt% platinum shown as an example) showed generally well-distributed platinum particles on the CNF surface, although a partial particles agglomeration could be observed. This

Table 1
Prepared ME As with sedimented CNF-electrodes. The anode and the cathode of each MEA are similar in design and have a platinum content of 0.7 mg cm^{-2}.

CNF content of the GDL [mg cm^{-2}]	PTFE-content of the GDL [wt%]	CNF content of the AL [mg cm^{-2}]	Platinum loading of the CNFs [wt%]
MEAs investigated for the optimisation of the AL-thickness and the binder content of the GDL			
6.6	21	4.7	13
6.6	21	3.5	17
6.6	21	2.9	19
6.6	21	2.5	22
6.6	21	2.2	24
6.6	15	4.7	13
6.6	15	3.5	17
6.6	15	2.9	19
6.6	30	4.7	13
6.6	30	3.5	17
6.6	30	2.9	19
MEAs investigated for the optimisation of the GDL-thickness			
4.6	21	2.9	19
6.6	21	2.9	19
9.9	21	2.9	19
12.3	21	2.9	19

Table 2
The lowering of the platinum content of the MEAs was carried out with a constant CNF loading of the AL or a constant platinum loading of the CNFs used in the AL.

CNF content of the AL [mg cm^{-2}]	Platinum loading of the AL [mg cm^{-2}]	Platinum loading of the CNFs [wt%]
Optimised electrode with 0.7 mg cm^{-2} platinum		
2.9	0.7	19
Electrodes with a lower platinum content -constant CNF loading of the AL:		
Cathodes		
2.9	0.4	12
Anodes		
2.9	0.4	12
2.9	0.2	6.5
2.9	0.1	3.3
Electrodes with a lower platinum content -constant platinum loading of the CNFs used in the AL:		
Cathodes		
1.7	0.4	19
Anodes		
1.7	0.4	19
0.83	0.2	19
0.41	0.1	19

agglomeration increased the average platinum particle size to about 5–10 nm.

3.2. Electrode and MEA preparation

The fast and simple sedimentation process allowed the preparation of a thin dispersion of the CNF material and the binder. This assured a very good distribution of the electrode components and enabled an exact setting of the required amount of CNFs and binder and a uniform electrode thickness even in lab scale. Fig. 4 shows an SEM image of a sedimented electrode in an outside-margin position, where the individual layers can be seen. In the previous study, it had been observed that the CNFs and the binder structured a spa-

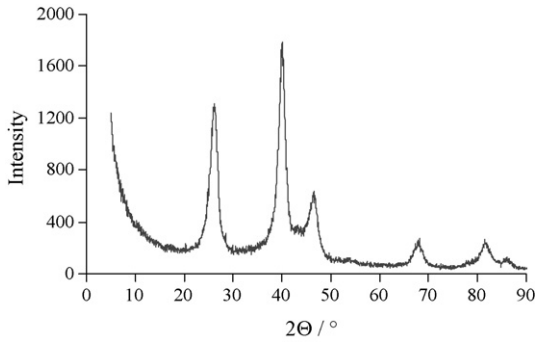

Fig. 1. X-ray diffraction results of CNFs loaded with 17 wt% platinum.

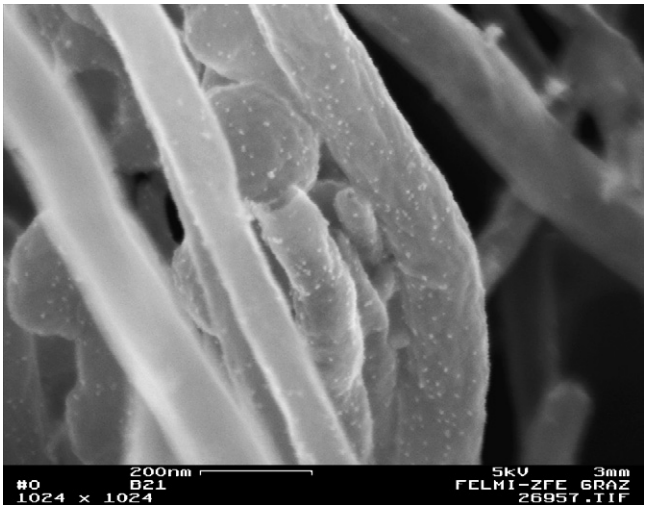

Fig. 2. SEM image of CNFs loaded with 19 wt% platinum.

Table 3
X-ray diffraction data of CNFs loaded with 17 wt% platinum.

	Profile widths broadened* [° 2Θ]	Broadening strain [°2Θ]	Peak position [°2Θ]	Crystallite size [nm]
Graphite	1.809	1.906	26.027	4.5
Pt	1.761	1.858	39.955	4.8
Graphite	1.989	2.087	43.724	4.3
Pt	1.885	1.982	46.431	4.6
Pt	2.074	2.172	67.806	4.6
Pt	2.896	2.994	81.540	3.6

* Profile widths standard 0.100° 2Θ.

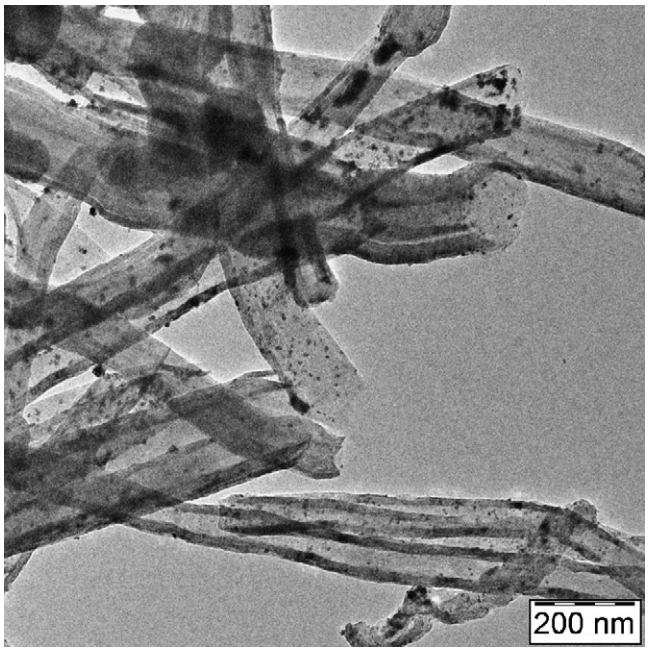

Fig. 3. TEM image of CNFs loaded with 19 wt% platinum.

cious pore system in the electrode. The low AL binder content gave stability without covering large surface areas of the catalyst support [28]. The thicknesses of both the GDL and the AL were controlled with the CNF loading per cm^2 that was in the range between 20 and 24 μm per mg cm^{-2} CNFs, becoming thicker with an increasing binder content. The spraying of the Nafion electrolyte on the AL side of the electrode resulted in a Nafion content of 33 ± 5 wt%, which should result in an optimum loading for PEMFC electrodes.

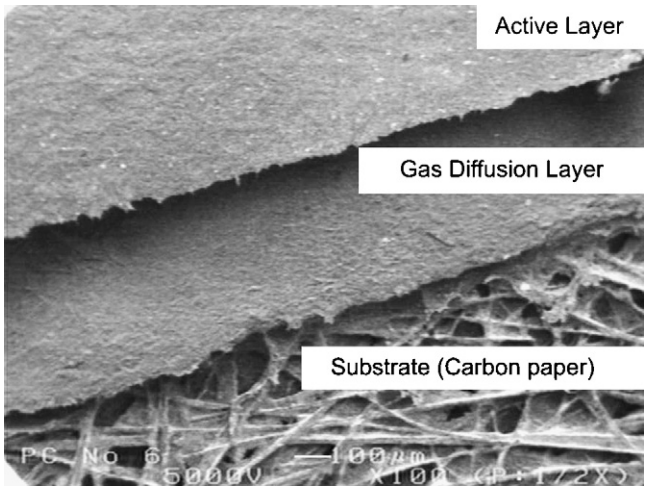

Fig. 4. SEM image of a sedimented CNF electrode in an outside-margin position.

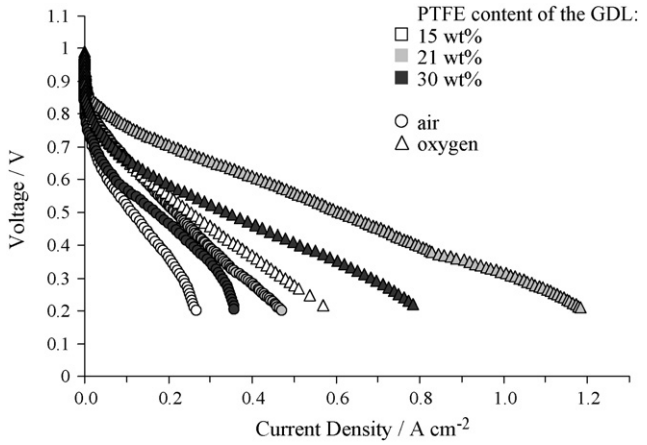

Fig. 5. Influence of the GDL binder content on the polarisation curves of the MEAs with air and oxygen (GDL: 6.6 mg cm^{-2} CNFs, AL: 3.5 mg cm^{-2} CNFs).

The deviation of 5 wt% was not expected to significantly influence the performance of the electrodes [41].

3.3. Influence of the PTFE content of the GDL on MEA performance

The binder content influences the structure of the electrode and the wetting behaviour of the GDL and therefore the water management and gas diffusion. To investigate the influence of the PTFE content of the GDL on the MEA performance, it was varied by using 15, 21 and 30 wt% of the CNF loading. This variation was carried out on electrodes with different AL thicknesses (2.9, 3.5 and 4.7 mg cm^{-2} CNFs; see Table 1). In this optimisation step, the GDL thickness was kept constant at 6.6 mg cm^{-2} CNFs. Fig. 5 shows the polarisation curves on the MEAs with a CNF content of the AL of 3.5 mg cm^{-2} as an example, and Fig. 6 shows the effect of the binder content on the maximum power density. These results clearly showed that in the case of different AL thicknesses, the electrodes with a GDL binder content of 21 wt% showed the best performance with air and oxygen. The lowering of the binder content down to 15 wt% resulted in a loss of performance, especially with oxygen. A possible reason for this may be that the larger amount of product water produced with oxygen as an oxidant could not be sufficiently removed because of the low hydrophobicity of the GDL. An increase in the binder content up to 30 wt% often resulted in a performance limited by gas diffusion, indicating a suboptimal pore structure of the GDL.

3.4. Influence of the AL thickness on MEA performance

Considering the AL thickness controlled by the CNF loading, the results in Fig. 6 show that the MEAs consisting of electrodes loaded with 2.9 mg cm^{-2} CNFs in the AL showed a better performance when compared to those with thicker ALs. Therefore, MEAs with thinner ALs (2.5 and 2.2 mg cm^{-2} CNFs; see Table 1) were investigated. The polarisation curves of the MEAs with different AL

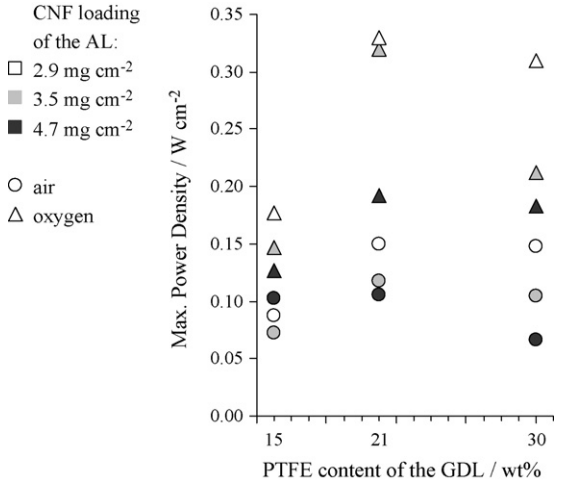

Fig. 6. Influence of the GDL binder content on the maximum power density of the MEAs with air and oxygen (GDL: 6.6 mg cm^{-2} CNFs).

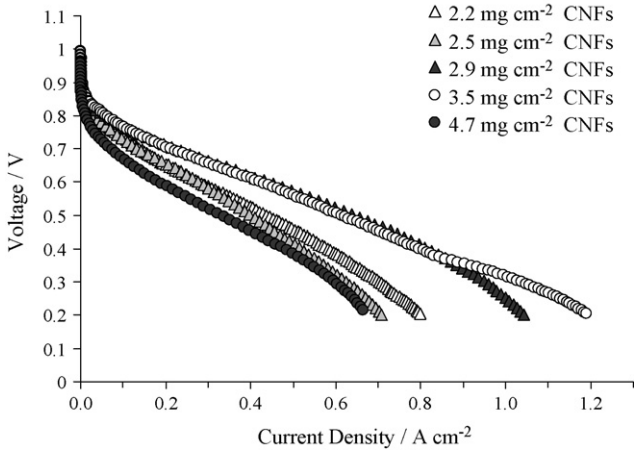

Fig. 7. Influence of the CNF loading of the AL on the polarisation curves of the MEAs with oxygen (GDL: 21 wt% PTFE and 6.6 mg cm^{-2} CNFs).

thicknesses but the same GDL (6.6 mg cm^{-2} CNFs and 21 wt% PTFE) are shown in Fig. 7. The polarisation curves and the comparisons in terms of maximum power densities relative to the MEAs with different AL thicknesses and GDL binder contents clearly show that the MEAs with ALs containing 2.9 mg cm^{-2} CNF performed best when compared to those with thicker or thinner ALs (see Fig. 8). This optimum in the performance could be caused either by an ideal platinum loading of the CNFs or by an ideal electrode thickness, which formed an optimal reactive zone. These two possible explanations for an optimum AL were investigated by lowering the catalyst loading of the electrodes.

3.5. Influence of the GDL thickness on MEA performance

The GDL thickness was optimised by varying its CNF loading. The GDL binder content (21 wt% PTFE) and the AL thickness (2.9 mg cm^{-2} CNFs) were kept constant (see Table 1). A lowering of the GDL thickness from 6.6 to 4.6 mg cm^{-2} CNFs resulted in a lower performance, but an increase up to 12.3 mg cm^{-2} CNFs led to an improvement, especially at higher current densities (see Fig. 9). The ohmic resistance of the MEAs was not significantly influenced by the GDL thickness. Fig. 10 shows a linear behaviour of the maximum power densities of the MEAs as a function of the CNF loading of their GDLs within an experimental error. These results indicate improved

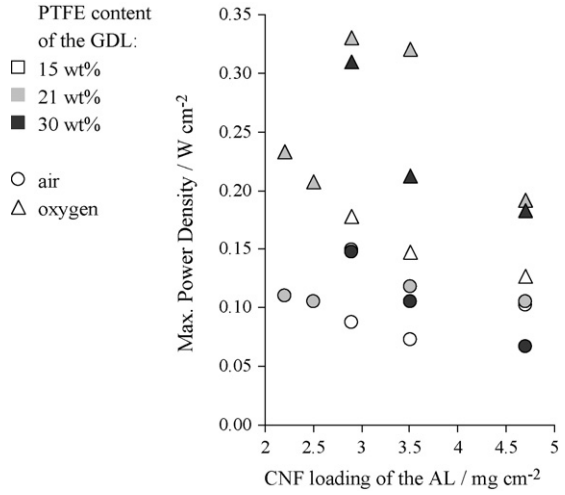

Fig. 8. Influence of the CNF loading of the AL on the maximum power density of the MEAs with air and oxygen (GDL: 6.6 mg cm^{-2} CNFs).

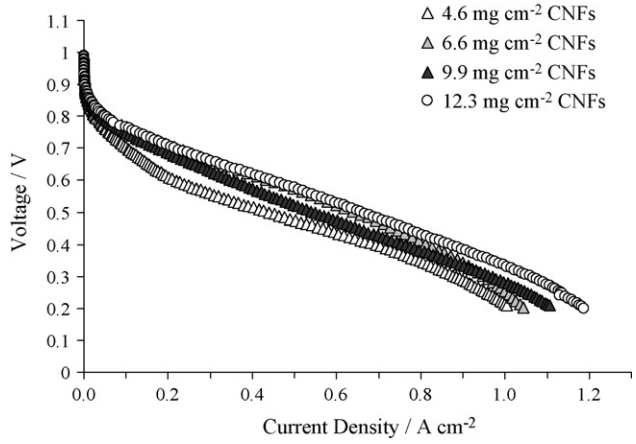

Fig. 9. Influence of the CNF loading of the GDL on the polarisation curves of the MEAs with oxygen (GDL: 21 wt% PTFE; AL: 2.9 mg cm^{-2} CNFs).

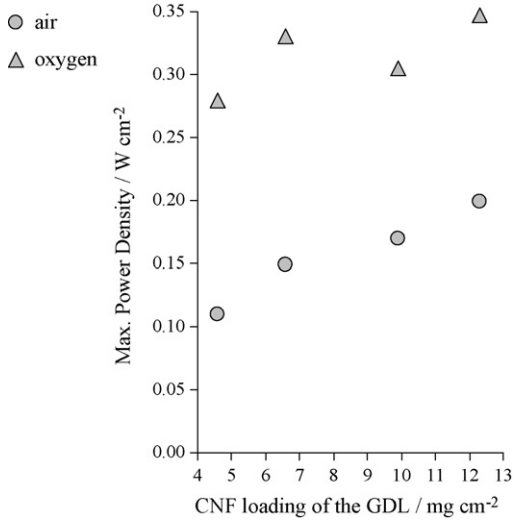

Fig. 10. Influence of the CNF loading of the GDL on the maximum power density of the MEAs with air and oxygen (GDL: 21 wt% PTFE; AL: 2.9 mg cm^{-2} CNFs).

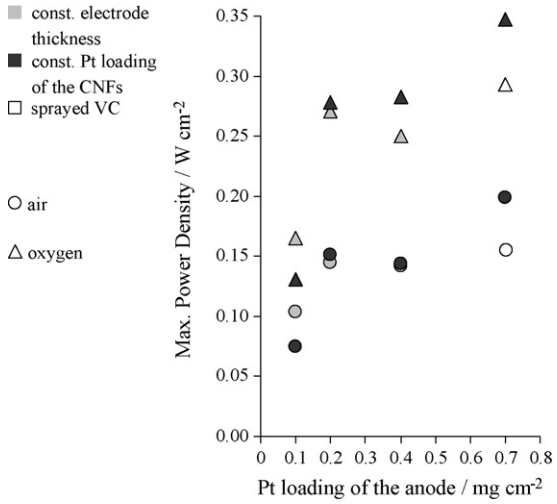

Fig. 11. Influence of the anode platinum loading on the maximum power density of CNF based MEAs with air and oxygen (GDL: 21 wt% PTFE, 12.3 mg cm^{-2} CNFs; AL: constant platinum loading of the CNFs, see Table 2). For comparison, the maximum power density of a MEA with sprayed Vulcan carbon (VC) based electrodes is shown.

gas and water management in thicker GDLs. Even though this trend was expected to continue, a further increase in the GDL thickness was not investigated because the sedimentation process could no longer ensure a uniform GDL thickness at higher CNF loadings.

3.6. Lowering of the catalyst loading of the electrodes

As expected, the lowering of the catalyst loading resulted in a lower performance, whereas the performance loss when lowering the anode catalyst loading from 0.4 to 0.2 mg cm^{-2} was rather moderate in both cases (constant platinum loading of the CNFs used in the AL or constant CNF loading of the AL; see Table 2). This is shown in Fig. 11. An anode catalyst loading of 0.1 mg cm^{-2} led to a rather high performance loss because of the low platinum loading of the CNFs used in the AL (3.3 wt%) or because of the small amount of platinum-loaded CNFs (0.41 mg cm^{-2}). Furthermore, the difference in the performance between two possibilities of lowering the catalyst loading was relatively small, but the MEAs with a constant platinum loading of the CNFs showed a better performance. Polarisation curves of these electrodes with oxygen are shown in Fig. 12.

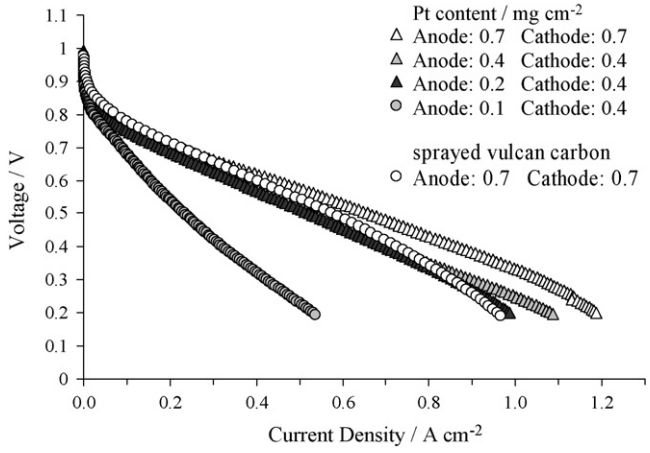

Fig. 12. Influence of the lowering of the platinum content on the polarisation curves of CNF based MEAs with oxygen (GDL: 21 wt% PTFE, 12.3 mg cm^{-2} CNFs; AL: constant platinum loading of the CNFs, see Table 2). For comparison, the polarisation curve of a MEA with sprayed Vulcan carbon based electrodes is shown.

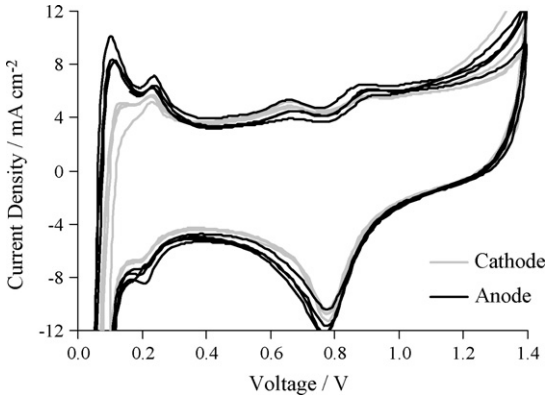

Fig. 13. CVs of a CNF based MEA (GDL: 21 wt% PTFE, 6.6 mg cm^{-2} CNFs; AL: 2.9 mg cm^{-2} CNFs, 0.7 mg cm^{-2} platinum).

For comparison, the polarisation curve and the maximum power density of the MEA consisting of sprayed Vulcan carbon electrodes is shown in Figs. 11 and 12, whereas the same type and the same amount of electrolyte was used as in the case of MEAs with CNF-based electrodes. These results showed that the CNF-based MEA with the same catalyst loading clearly performed better, especially at higher current densities, indicating an improved gas distribution in the CNF-based electrodes.

The specific active catalyst surface of the anodes of these MEAs was calculated from the CVs using the following equations:

$$S_{\mathrm{act}} = \frac{Q_{\mathrm{T}} 0.1}{Q_{\mathrm{H}} l_{\mathrm{Pt}}} \tag{1}$$

$$Q_{\mathrm{T}} = \frac{1}{\upsilon} \int_{dE} (i_{\mathrm{d}} - i_{\mathrm{a}}) dE \tag{2}$$

where S_{act} [m^2 g^{-1}] is the specific active surface of the platinum deposited on the CNFs, Q_{T} [C cm^{-2}] is the total charge transfer density in the hydrogen adsorption/desorption potential region between ~0.05 V and the beginning of the double layer region at ~0.45 V, Q_{H} [210×10^{-6} C cm^{-2}] is the charge density of platinum with monolayer adsorption of hydrogen, and l_{Pt} [mg cm^{-2}] is the specific catalyst loading of the electrode. Q_{T} is calculated by the integration of the CV curves in the adsorption/desorption potential region dE [V], where υ is the scan rate [V s^{-1}], and i_{d} [A cm^{-2}] and i_{a} [A cm^{-2}] are the current densities of desorption and adsorption [42].

Fig. 13 exemplifies the CVs of an MEA with CNF-based electrodes. The CVs of the cathodes of all the investigated MEAs showed that one of the two hydrogen adsorption peaks expected to be observed clearly was significantly smaller than this peak of the anode CV, even if the platinum loading of the anode and the cathode was the same. Therefore, the calculated active surface of the cathode was lower. We have no exact explanation for this observation; it might indicate impurities in the oxygen or in the synthetic air, or the beginning of cathode corrosion.

The specific active platinum surfaces of the anodes in Fig. 14 showed that the highest utilisation of the anode catalyst was reached at a platinum loading of between 0.2 and 0.4 mg cm^{-2}, but not at the high platinum loading of 0.7 mg cm^{-2}, even though the concerning MEA performed better. The low active platinum surface of one of the anodes, with a platinum loading of 0.4 mg cm^{-2}, was supposed to be an outlier. The platinum utilisation of the anodes started to decrease drastically at a platinum loading below 0.2 mg cm^{-2}. The difference in the platinum utilisation between the two different kinds of electrodes at the same platinum loading was rather small, indicating that negative effects on the performance occur when lowering the AL thickness and

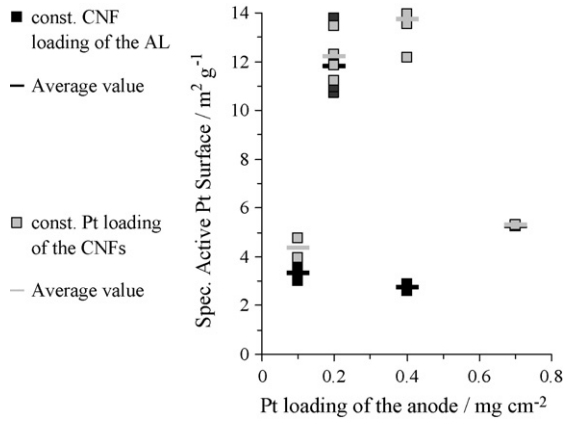

Fig. 14. Influence of the lowering of the platinum content on the specific active platinum surfaces of the anodes (GDL: 21 wt% PTFE, 12.3 mg cm^{-2} CNFs; AL: see Table 2).

when lowering the platinum loading of the catalyst support as well.

4. Conclusions

In the presented work, we investigated tubular carbon nanofibers with an average diameter of 150 nm as electrode material for the gas diffusion layer and the catalyst support for PEMFCs. Well-dispersed platinum particles with an average crystallite size of 4.6 nm and an average particle diameter of 5–10 nm were deposited on surface-oxidised fibers with an electroless plating method in aqueous media. The carbon nanofiber-based electrodes were prepared by a time-efficient and simple sedimentation process, which allowed the preparation of a thin dispersion of the CNF material and binder. This assured a very good distribution of the components and enabled an exact setting of the required amount of CNFs, binder and catalyst support and a uniform electrode thickness, even in lab scale. The electrodes were optimised by varying the thickness of the gas diffusion layer and its binder content as well as the thickness of the active layer. These optimised electrodes performed considerably better than Vulcan carbon based electrodes with the same catalyst loading prepared by a spraying process using the same type and amount of electrolyte in the membrane electrode assembly. By reducing the platinum content from 0.7 to 0.2 mg cm^{-2}, catalyst utilisation was significantly increased.

Acknowledgements

The authors acknowledge the support of the Christian Doppler Society, Vienna, the Austrian Ministry of Innovation and Technology (BMVIT, A3 programme), Vienna and Electrovac AG, Klosterneuburg. We also thank Assunta Patti from CNR-ITAE for her helpful contributions to our work.

References

[1] Z. Liu, X. Lin, J.Y. Lee, W. Zhang, M. Han, L.M. Gan, Langmuir 18 (2002) 4054–4060.
[2] F. Yuan, H.K. Yu, H. Ryu, Electrochim. Acta 50 (2004) 685–691.
[3] Z. Liu, L.M. Gan, L. Hong, W. Chen, J.Y. Lee, J. Power Sources 139 (2004) 73–78.
[4] T. Matsumoto, T. Komatsu, H. Nakano, K. Arai, Y. Nagashima, E. Yoo, T. Yamazaki, M. Kijima, H. Shimizu, Y. Takasawa, J. Nakamura, Catal. Today 92 (2004) 277–281.
[5] T. Matsumoto, T. Komatsu, K. Arai, T. Yamazaki, M. Kijima, H. Shimizu, Y. Takasawa, J. Nakamura, Chem. Commun. (2004) 840–841.
[6] M. Gangeri, G. Centi, A. La Malfa, S. Perathoner, R. Vieira, C. Pham-Huu, M.J. Ledoux, Catal. Today 102–103 (2005) 50–57.
[7] Z.R. Ismagilov, M.A. Kerzhentsev, N.V. Shikina, A.S. Lisitsyn, L.B. Okhlopkova, C.N. Barnakov, M. Sakashita, T. Iijima, K. Tadokoro, Catal. Today 102–103 (2005) 58–66.
[8] N. Rajalakshmi, H. Ryu, M.M. Shaijumon, S. Ramaprabhu, J. Power Sources 140 (2005) 250–257.
[9] J.M. Tang, K. Jensen, M. Waje, W. Li, P. Larsen, K. Pauley, Z. Chen, P. Ramesh, M.E. Itkis, Y. Yan, R.C. Haddon, J. Phys. Chem. C 111 (2007) 17901–17904.
[10] M. Gangeri, S. Perathoner, G. Centi, Inorg. Chim. Acta 359 (2006) 4828–4832.
[11] M.S. Saha, R. Li, X. Sun, J. Power Sources 177 (2008) 314–322.
[12] C. He, H.R. Kunz, J.M. Fenton, J. Electrochem. Soc. 144 (1997) 970–979.
[13] C.A. Bessel, K. Laubernds, N.M. Rodriguez, R.T.K. Baker, J. Phys. Chem. B 105 (2001) 1115–1118.
[14] E.S. Steigerwalt, G.A. Deluga, D.E. Cliffel, C.M. Lukehart, J. Phys. Chem. B 105 (2001) 8097–8101.
[15] E.S. Steigerwalt, G.A. Deluga, C.M. Lukehart, J. Phys. Chem. B 106 (2002) 760–766.
[16] W. Li, C. Liang, J. Qiu, W. Zhou, H. Han, Z. Wei, G. Sun, Q. Xin, Carbon 40 (2002) 791–794.
[17] W. Li, C. Liang, W. Zhou, J. Qiu, Z. Zhou, G. Sun, Q. Xin, J. Phys. Chem. B 107 (2003) 6292–6299.
[18] W. Li, C. Liang, W. Zhou, J. Qiu, Z. Zhou, J. Qiu, H. Li, G. Sun, Q. Xin, Carbon 42 (2004) 436–439.
[19] G. Girishkumar, K. Vinodgopal, P.V. Kamat, J. Phys. Chem. B 108 (2004) 19960–19966.
[20] X. Li, S. Ge, C.L. Hui, I.M. Hsing, Electrochem, Solid State Lett. 7 (2004) A286–A289.
[21] X. Li, W.X. Chen, J. Zhao, W. Xing, Z.D. Xu, Carbon 43 (2005) 2168–2174.
[22] E. Frackowiak, G. Lota, T. Cacciaguerra, F. Béguin, Electrochem. Commun. 8 (2006) 129–132.
[23] C.H. Wang, H.Y. Du, Y.T. Tsai, C.P. Chen, C.J. Huang, L.C. Chen, K.H. Chen, H.C. Shih, J. Power Sources 171 (2007) 55–62.
[24] V. Selvaraj, M. Alagar, Electrochem. Commun. 9 (2007) 1145–1153.
[25] J. Cao, C. Du, S.C. Wang, P. Mercier, X. Zhang, H. Yang, D.L. Akins, Electrochem. Commun. 9 (2007) 735–740.
[26] M. Tsuji, M. Kubokawa, R. Yano, N. Miyamae, T. Tsuji, M.S. Jun, S. Hong, S. Lim, S.H. Yoon, I. Mochida, Langmuir 23 (2007) 387–390.
[27] V. Hacker, E. Wallnöfer, W. Baumgartner, T. Schaffer, J.O. Besenhard, H. Schröttner, M. Schmied, Electrochem. Commun. 7 (2005) 377–382.
[28] E. Wallnöfer, W. Baumgartner, T. Schaffer, J.O. Besenhard, V. Hacker, ECS Trans 1 (6) (2006) 491–499.
[29] X. Zhao, W. Li, L. Jiang, W. Zhou, Q. Xin, B. Yi, G. Sun, Carbon 42 (2004) 3263–3265.
[30] X. Li, I.M. Hsing, Electrochim. Acta 5 (2006) 5250–5258.
[31] X. Sun, R. Li, D. Villers, J.P. Dodelet, S. Désilets, Chem. Phys. Lett. 379 (2003) 99–104.
[32] B. Xue, P. Chen, Q. Hong, J. Lin, K.L. Tan, J. Mater. Chem. 11 (2001) 2378–2381.
[33] M.L. Toebes, M.K. van der Lee, L.M. Tang, M.H. Huis in't Veld, J.H. Bitter, A.J. van Dillen, K.P. de Jong, J. Phys. Chem. B 108 (2004) 11611–11619.
[34] Y. Xing, J. Phys. Chem. B 108 (2004) 19255–19259.
[35] V. Lordi, N. Yao, J. Wei, Chem. Mater. 13 (2001) 733–737.
[36] Z. Liu, J.Y. Lee, W. Chen, M. Han, L.M. Gan, Langmuir 20 (2004) 181–187.
[37] M.K. van der Lee, A.J. van Dillen, J.H. Bitter, K.P. de Jong, J. Am. Chem. Soc. 127 (2005) 13573–13582.
[38] V. Ramani, H.R. Kunz, J.M. Fenton, J. Membrane Sci. 279 (2006) 506–512.
[39] T.W. Ebbesen, J. Phys. Chem. Solids 57 (1996) 951–955.
[40] R. Yu, L. Chen, Q. Liu, J. Lin, K.L. Tan, S.C. Ng, H.S.O. Chan, G.C. Xu, T.S.A. Hor, Chem. Mater. 10 (1998) 718–722.
[41] E. Passalacqua, F. Lufrano, G. Squadrito, A. Patti, L. Giorgi, Electrochim. Acta 46 (2001) 799–805.
[42] W. Vielstich, in: W. Vielstich, H. Gasteiger, A. Lamm (Eds.), Handbook of Fuel Cells - Fundamentals, Technology and Applications, vol. 2, Cyclic Voltammetry, John Wiley & Sons Ltd., West Sussex, 2003, pp. 153–162, Chapter 14.